

# UC San Diego

## UC San Diego Previously Published Works

### Title

Direct Generation of Human Cortical Organoids from Primary Cells

### Permalink

<https://escholarship.org/uc/item/58g4g12g>

### Journal

Stem Cells and Development, 27(22)

### ISSN

1547-3287

### Authors

Schukking, Monique  
Miranda, Helen C  
Trujillo, Cleber A  
[et al.](#)

### Publication Date

2018-11-15

### DOI

10.1089/scd.2018.0112

Peer reviewed

# Direct Generation of Human Cortical Organoids from Primary Cells

Monique Schukking,<sup>1,2</sup> Helen C. Miranda,<sup>1,2</sup> Cleber A. Trujillo,<sup>1,2</sup>  
Priscilla D. Negraes,<sup>1,2</sup> and Alysson R. Muotri<sup>1-4</sup>

The study of variations in human neurodevelopment and cognition is limited by the availability of experimental models. While animal models only partially recapitulate the human brain development, genetics, and heterogeneity, human-induced pluripotent stem cells can provide an attractive experimental alternative. However, cellular reprogramming and further differentiation techniques are costly and time-consuming and therefore, studies using this approach are often limited to a small number of samples. In this study, we describe a rapid and cost-effective method to reprogram somatic cells and the direct generation of cortical organoids in a 96-well format. Our data are a proof-of-principle that a large cohort of samples can be generated for experimental assessment of the human neural development.

**Keywords:** induced pluripotent stem cell, organoids, high-throughput, neural development

## Introduction

THE LIMITED AVAILABILITY of relevant experimental models constrains the ability to study variations in human condition and disorders. The understanding of the etiological mechanisms underlying these variations is the basis of the progress of new treatments. Most of the neurodevelopmental disorders have a strong genetic component. For example, autism spectrum disorders (ASD) are a neuropsychiatric condition with heritability higher than 80% [1]. Nevertheless, the majority of the identified mutations are not highly penetrant and are often associated with multiple disorders [2]. To distinguish causal correlation from variants of unknown significant requires the study of the impact of genetic variants in multiple genetic backgrounds.

Noninvasive access to human brain tissue is restricted due to its fragile nature and ethical concerns. Even though postmortem tissue can provide information on alterations in the brain structure at a cellular and molecular level, it often represents the end stage of the disease. In addition, to derive causal interferences from pathological studies of neurodevelopmental disorders on postmortem tissues remains a challenge [2]. Although animal models can generate insights into brain development and the function of specific genes, they seldom replicate the genetic diversity of a patient [2]. Finally, aspects of the development, cell composition, structure, and electrophysiological properties of the brain of

animal models do not fully recapitulate the uniqueness of the human brain [3–6].

Since 2007, human-induced pluripotent stem cells (iPSCs) can be generated by transducing somatic cells with pluripotent factors, a process known as cellular reprogramming [7]. Then, through a specific combination of growth factors and cellular conditions, iPSCs can be further differentiated into glial cells, neurons, and other terminally differentiated cell types [8]. This technique facilitates the study of previously inaccessible live relevant human brain cells by capturing the genetic diversity of the patient *in vitro*.

The generation of stem cells from patients and their healthy relatives allows for the investigation of the genetic variants that either predisposed or protected them from disease conditions [9–11]. Until recently, a critical limitation of iPSCs to model neurological disorders was the lack of protocols allowing for the dynamic interaction among different cell types in a systematic and organized manner, mimicking human brain development.

Organoids are tridimensional cell clusters derived from pluripotent stem cells that are capable of self-renew and organize, while maintaining the genotype of the original cell or tissue source. Organoids have been established for many organs, including the brain [8]. There are now several distinct methods [12–15] to enable the development of a cerebral organoid system from human iPSCs [15,16]. These cerebral organoids are heterogeneous and form a variety of brain

<sup>1</sup>Department of Pediatrics, Rady Children's Hospital San Diego and <sup>2</sup>Stem Cell Program, Department of Cellular and Molecular Medicine, University of California San Diego School of Medicine, La Jolla, California.

<sup>3</sup>Kavli Institute for Brain and Mind and <sup>4</sup>Center for Academic Research and Training in Anthropogeny (CARTA), University of California San Diego, La Jolla, California.

regions, including ventral forebrain, cerebral cortex, hippocampus, and mid- and hindbrain boundary. They exhibit neurons that are functional and capable of electrical excitation [12–14]. These brain organoids also resemble human cortical development at the gene expression levels [17].

The primary advantage of brain organoids derived from iPSCs as a model is that starting with only a limited amount of material, for example, a biopsy of the skin, it allows for an in-depth analysis of neural networks, cell behavior, drug screening, disease modeling, and variations in brain development [8]. Also, organoids can facilitate host–microbe research: Infectious diseases, such as the Zika virus, can be modeled by introducing the microbes into the organoids [18–20].

However, the main limitation of the iPSC-derived brain organoid model is the high cost and time-consuming stage of cellular reprogramming. Studies using this approach are therefore often restricted to a small number of samples. High-throughput production of iPSCs followed by brain organoid generation would limit variation in production time and would, therefore, be groundbreaking in the usage of this model.

In this study, we describe a rapid and cost-effective method to reprogram individual somatic cells and to generate cortical organoids in a 96-well format directly. This method can be further optimized to generate brain organoids from hundreds of individuals simultaneously in a fully automated and systematic approach. Our data are a proof-of-principle that a large cohort of samples can be generated for experimental assessment of the variability of human cognition in both healthy and disease context.

## Materials and Methods

### *iPSCs generation*

Fibroblasts from a control individual were reprogrammed using Yamanaka factors in Sendai Virus Kit (Cytotune™ iPSC; Invitrogen) composed of 2.0 hKOS, containing human *KLF4*, *OCT3/4*, and *SOX2*; 2.0 hKlf4, containing human *KLF4*, and 2.0 hc-Myc, containing human *c-Myc*. Cells were cultured in Dulbecco's modified Eagle's medium/Ham's F12 (DMEM/F12 50/50; Corning) with glutamine, 10% fetal bovine serum (FBS), and 1% penicillin–streptomycin. Two days before transduction, the medium was changed to DMEM, 15% FBS, and 1% penicillin–streptomycin.

One day before transduction, 50,000 cells per well were seeded in a 6-well plate; or 500, 1,000, 5,000, or 10,000 cells per well in a 96-well plate. In the six-well plate, cells were transduced with 18.5  $\mu\text{L}/\text{mL}$  of each of the factors in Sendai virus (2.0 hKOS, 2.0 hKlf4, and 2.0 hc-Myc) in 1 mL DMEM with 5% FBS. In the 96-well plate, cells were transduced with 1.0, 2.8, 5.7, or 11.3  $\mu\text{L}/\text{mL}$  of each of the factors in the Sendai virus, in 100  $\mu\text{L}$  DMEM with 5% FBS. One day after transduction, the medium was changed to DMEM with 10% FBS.

Two days after transduction, feeder cells were seeded on top of the fibroblasts: In the six-well plate, we seeded 131,950 mouse embryonic fibroblasts (MEFs) per well, and in the 96-well plate, we seeded 5,000 MEFs per well. After 24 h, daily media changes were performed using human embryonic stem cell media, which contains DMEM/F12 with glutamine, 20% knockout serum, 1% nonessential amino acids (NEAA), 0.2%  $\beta$ -mercaptoethanol, and 33.3  $\eta\text{g}/\text{mL}$  basic fibroblast growth factor (bFGF; Life Technologies).

Four days after transduction, cells were treated for 5 days with 1  $\mu\text{M}$  valproic acid to promote chromatin relaxation and increased transduction efficiency. Five days after adding the feeder cells, HUES media was switched to HUES media conditioned with MEFs. iPSC colonies started to form after ~14 days. This study was approved by the University of California San Diego IRB/ESCRO committee (protocol 141223ZF).

### *Cortical organoid generation*

Human iPSC-derived cortical organoids were generated as previously described [15,21], using ultralow attachment 96-well plate (Costar): Day 0: One hour before dissociation of the iPSCs, cells were treated with 10  $\mu\text{M}$  Y-27632, which is a Rho-associated protein kinase (ROCK) inhibitor. Cells were washed twice with 100  $\mu\text{L}$  phosphate-buffered saline (PBS) and then twice with 100  $\mu\text{L}$  Accutase in PBS (1:1; Life Technologies). After 10–20 min, dissociated cells were resuspended in 150  $\mu\text{L}$  media containing mTeSR1 (Stem Cell Technologies), 10  $\mu\text{M}$  SB431542 (Stemgent), 1  $\mu\text{M}$  dorsomorphin (R&D System), and 5  $\mu\text{M}$  Y-27632 ROCK inhibitor, and passed through a moistened 40  $\mu\text{m}$  cell strainer.

Cells were transferred to two wells of an ultralow attachment 96-well plate (Costar), volumes were increased to 100–150  $\mu\text{L}$  per well, and cells were kept under suspension at 95 rpm, at 37°C and 5% CO<sub>2</sub>. Organoids formed after 2–3 days. Day 1–2: Media was changed to mTeSR1 with 10  $\mu\text{M}$  SB431542 (Stemgent) and 1  $\mu\text{M}$  dorsomorphin (R&D System). The cells were kept in this media for 2 days. Due to the low volume in each well, media was changed every day during the entire protocol.

Day 3–8: For neural induction, Neurobasal (Gibco) media without L-glutamine containing 1% N2 NeuroPlex (Gemini Bio-Products), 2% Gem21 NeuroPlex (Gemini Bio-Products), 1% NEAA, 1% Glutamax, 1% penicillin–streptomycin, 1  $\mu\text{M}$  dorsomorphin (R&D System), and 10  $\mu\text{M}$  SB431542 (Stemgent) was used for 6 days. Day 9–15: For 7 days, neural progenitor cell (NPC) proliferation was obtained in the presence of Neurobasal (Gibco) media without L-glutamine supplemented with 2% Gem21 NeuroPlex (Gemini Bio-Products), 1% NEAA, 1% Glutamax, 1% penicillin–streptomycin, and 20  $\eta\text{g}/\text{mL}$  bFGF. Day 16–21: NPC proliferation was continued for another 6 days with the addition of 20  $\eta\text{g}/\text{mL}$  epidermal growth factor.

Day 22–27: During the following 6 days, organoids were maintained in Neurobasal (Gibco) media without L-glutamine supplemented with 2% Gem21 NeuroPlex (Gemini Bio-Products), 1% NEAA, 1% Glutamax, 1% penicillin–streptomycin, 10  $\eta\text{g}/\text{mL}$  brain-derived neurotrophic factor, 10  $\eta\text{g}/\text{mL}$  glial cell-derived neurotrophic factor, 10  $\eta\text{g}/\text{mL}$  neurotrophin-3, 200  $\mu\text{M}$  ascorbic acid, and 1 mM dibutyryl-cAMP to speed up neuronal maturation. During the whole protocol, we changed media every day to make sure that, despite the smaller volume of media that fits in the well, the organoids would not be depleted of any growth factor.

### *Quantitative reverse transcription–polymerase chain reaction analysis*

The expression of pluripotency markers in iPSCs was assessed by quantitative reverse transcription–polymerase chain reaction (RT-qPCR). RNA was obtained from iPSC colonies of 5 wells of the 96-well plate using the RNeasy

Plus Micro Kit (Qiagen). We generated 40  $\mu$ L cDNA from 378 ng of RNA using the QuantiTect Reverse Transcription Kit (Qiagen), and 2  $\mu$ L of cDNA was used in each RT-qPCR assay using TaqMan probes and TaqMan Universal Master Mix II (Life Technologies). *HPRT* was used as a house-keeping gene, and the reactions were performed in triplicates.

#### Immunofluorescence analysis

We examined if the formed cortical organoids consisted of neuronal cells. We immunostained for NESTIN; a marker for NPCs and MAP2; and a marker for neural differentiation. To do this, we first spread out the cells of the cortical organoids: At day 24, 22, or 17 of the cortical organoid protocol, the organoids were plated in a “Lab Trek II

chamber slide with cover RS glass slide” that was previously coated for 24 h in Matrigel. Cortical organoids were grown on these slides for 2–3 days in Neurobasal (Gibco) media without L-glutamine supplemented with 2% Gem21 NeuroPlex (Gemini Bio-Products), 1% NEAA, 1% Gluta-max, and 1% penicillin–streptomycin.

Then, we performed immunofluorescence staining as follows: cells were washed once with PBS and then fixed in 4% paraformaldehyde for 20 min at room temperature (RT). Washed once with PBS and permeabilized with 0.2% Triton X-100 for 20 min. After, they were incubated in blocking solution composed of 3% bovine serum albumin in PBS for 20 min at RT. After blocking, the organoids were incubated in primary antibodies mouse-anti-NESTIN (1:500) and chicken-anti-MAP2 (1:2,000) in blocking solution at +4°C overnight.

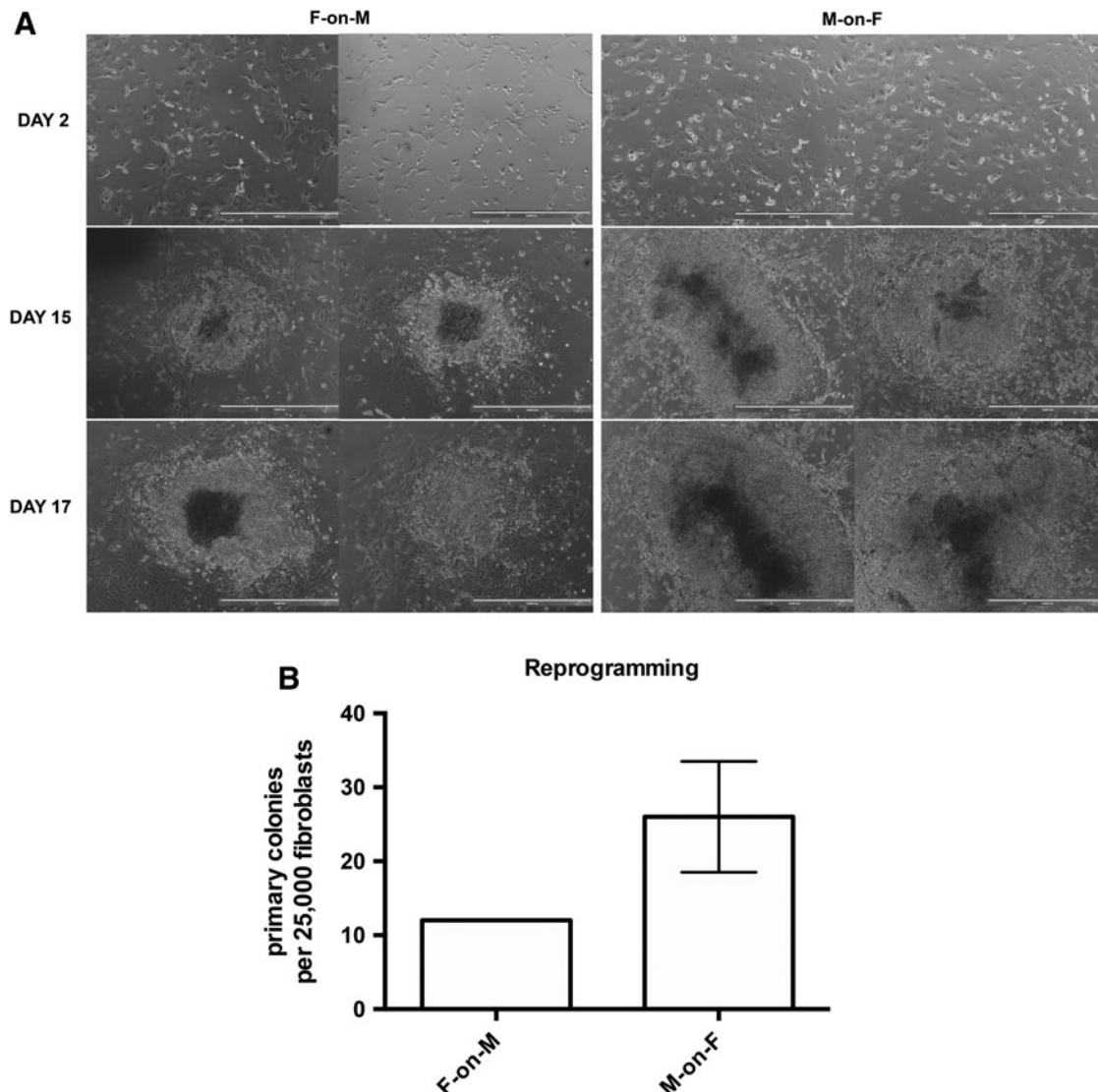


**FIG. 1.** MEFs facilitate the reprogramming process. **(A)** *Left* is human skin fibroblasts on top of MEFs (F-on-M) in a 10 cm disk and *right* is MEFs on top of human skin fibroblasts (M-on-F) in a six-well plate. Images made using EVOS microscope at 4 $\times$ . Scale bar, 1,000  $\mu$ m. (Day 2) Pictures were taken 2 days after transduction. F-on-M pictures just taken after reseeding fibroblasts on top of MEFs. M-on-F pictures just taken after seeding MEFs on top of fibroblasts. (Day 15) Pictures were taken 15 days after transduction. iPSC colonies started to show. (Day 17) Pictures were taken 17 days after transduction. **(B)** Relative number of primary colonies formed per 25,000 fibroblasts counted on reprogramming day 17. Results are presented as mean  $\pm$  SEM,  $n=2$ . The SEM for F-on-M is zero. EVOS, EVOS Cell Imaging Systems (ThermoFisher); iPSC, induced pluripotent stem cell; MEFs, mouse embryonic fibroblasts; SEM, standard error of the mean.

The next day, they were washed twice with PBS and incubated in secondary antibodies 488 anti-mouse (1:500) and 555 anti-chicken (1:500) in blocking solution for 1 h at RT. After 1 h, washed twice with PBS and stained nuclei by incubating in DAPI (1:10,000) in blocking solution for 10 min at RT. Finally, they were washed with PBS and slides were mounted using ProLong Gold antifade mountant (Life Technologies). Images were made on EVOS Cell Imaging Systems (ThermoFisher) at 4× magnification.

### Statistical analysis

All data are presented as the mean ± standard error of the mean. The statistical analyses were performed using Prism software (GraphPad, San Diego, CA). As indicated, unpaired Student's *t*-test followed by Welch's correction when variances were not equal was used. Significance was represented as <sup>ns</sup>*P* > 0.05, \**P* < 0.05, \*\**P* < 0.01, \*\*\**P* < 0.001, and \*\*\*\**P* < 0.0001.

## Results

### Optimization of reprogramming and direct differentiation into brain organoids

We started by establishing the optimal reprogramming conditions. Direct reprogramming in a feeder-free condition is notorious low efficient [22–24]. Moreover, traditional reprogramming strategies would require clonal selection of the original iPSC colonies into MEFs. To avoid these steps, we decided to seed MEFs directly onto the reprogramming wells after transduction to increase iPSCs survival.

We first optimized the conditions in a six-well plate to minimize the edge effect caused by well size. Fibroblasts were transduced using the four Yamanaka factors [7] using Sendai viruses. Two days after transduction, the seeding was performed in two different conditions: (1) the fibroblasts were seeded on top of MEFs and (2) MEFs on top of the fibroblasts. In both approaches, iPSC colonies formed approximately after 15 days (Fig. 1A). The data show that reprogramming was

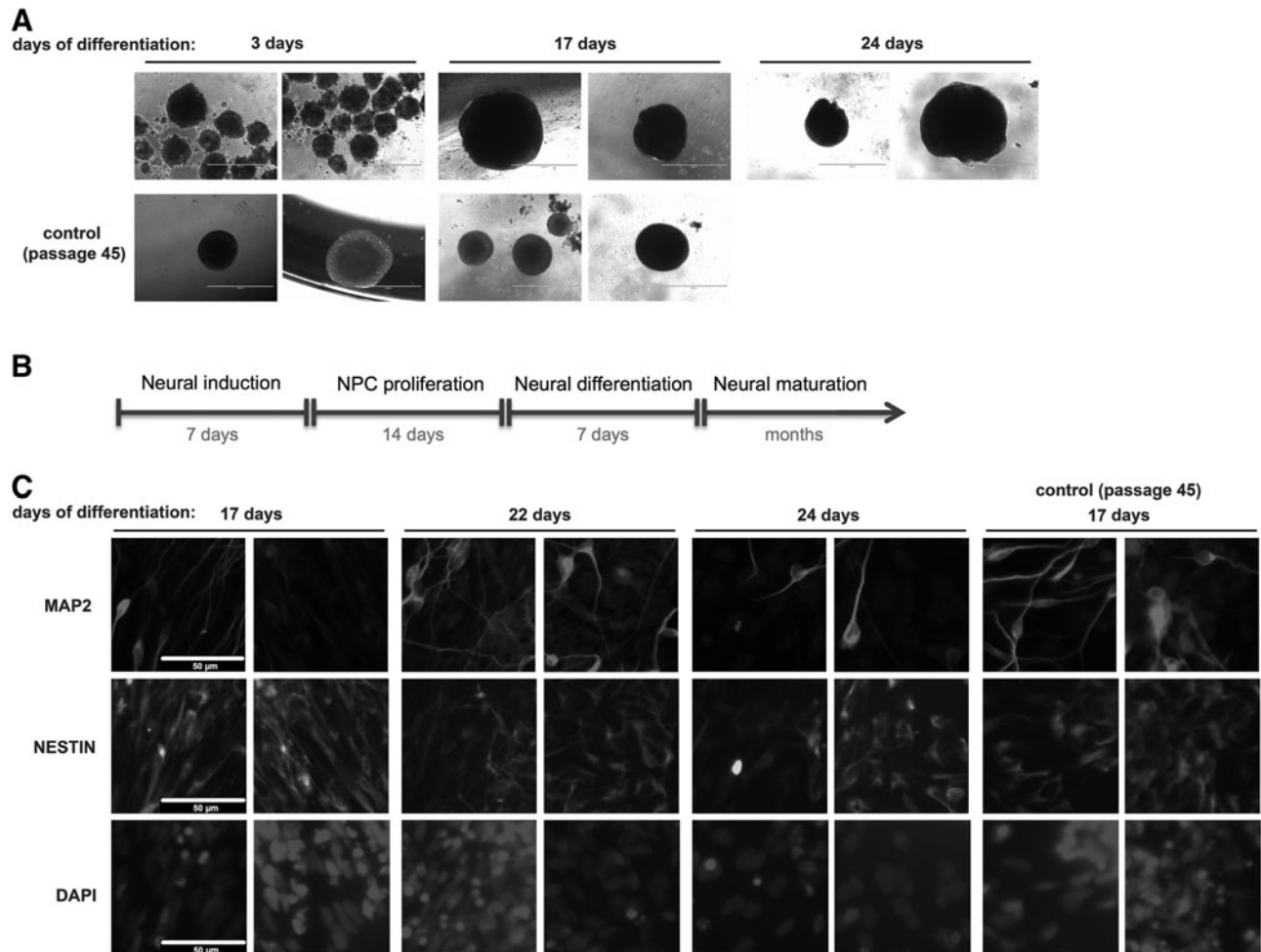


**FIG. 2.** Cortical organoids formed from nonpassaged iPSCs. The cortical organoid protocol was started in a 24-well plate using nonpassaged iPSCs at day 24 and 32 of the reprogramming protocol. To control for extensive cellular turnover, iPSCs of passage 45 were included. **(A)** Images of the organoids formed at protocol days 3, 17, and 24. Images made using EVOS at magnification 4×. Scale bar, 1,000 μm. **(B)** Graphical diagram of the protocol used to generate cortical organoids. **(C)** Cortical organoids stained for MAP2, a marker for neural differentiation, NESTIN, marker for NPCs and nuclei marker DAPI. Images made using EVOS at magnification 20×. Scale bar, 50 μm. NPCs, neural progenitor cells.

achieved whether fibroblasts were plated either on top or below MEF feeders. More experiments would be necessary to determine whether the reprogramming efficiency is improved on different plating conditions (Fig. 1B).

It has been reported that direct differentiation of iPSC colonies is challenging due to the extensive cellular turnover necessary to reach a fully reprogrammed state in iPSCs before directed neural differentiation [25,26]. This could be due to the epigenetic signature of the iPSC origin tissue, to the reprogramming strategy, and to similarities of the transcriptional profile [26–28]. To assess the feasibility to differentiate nonpassaged iPSCs immediately into cortical organoids, iPSCs were plated into a 24-well plate to minimize the edge effect caused by well size. The differentiation protocol was started using nonpassaged iPSC colonies from our previous experiment at day 24 and 32 of the reprogramming protocol. As a control for extensive cellular turnover, we included iPSCs at passage 45.

After only 3 days, we could already observe the formation of tridimensional structures (Fig. 2A). Figure 2B shows a schematic of the differentiation protocol. We confirmed the neural identity of these organoids by immunostaining for the NPCs, NESTIN, and the marker for neuronal cells, MAP2 (Fig. 2C). All organoids were positive for NESTIN and MAP2, confirming the presence of NPCs and neurons. Full

characterization with cortical layer structure immunostaining as well as cell PCR analysis of organoids formed by this cortical organoid protocol was demonstrated by Trujillo et al. [29]. Our results indicated that the nonpassaged iPSCs could potentially generate cortical organoids without previous expansion.

### Cortical organoids can be originated from fibroblasts reprogrammed in a 96-well plate

We previously established the optimal reprogramming conditions to form and maintain iPSCs by using MEF feeder cells. To establish the optimal reprogramming conditions, we started by plating human primary skin fibroblasts into a 96-well plate. Skin fibroblasts were seeded at four different concentrations. On the following day, a serial dilution of Sendai virus was added into the wells as described in Fig. 3A. The day after, 5,000 MEF feeder cells were seeded on top of each well to determine if the formed iPSC colonies instead could be maintained using MEF feeder cells.

Next, the number of iPSC colonies that appeared in the wells was evaluated over time. Colonies of iPSCs started to appear around day 14. At day 19, the iPSC colonies were still alive. As expected, these results indicate that seeding 5,000 MEFs directly into the reprogramming wells after

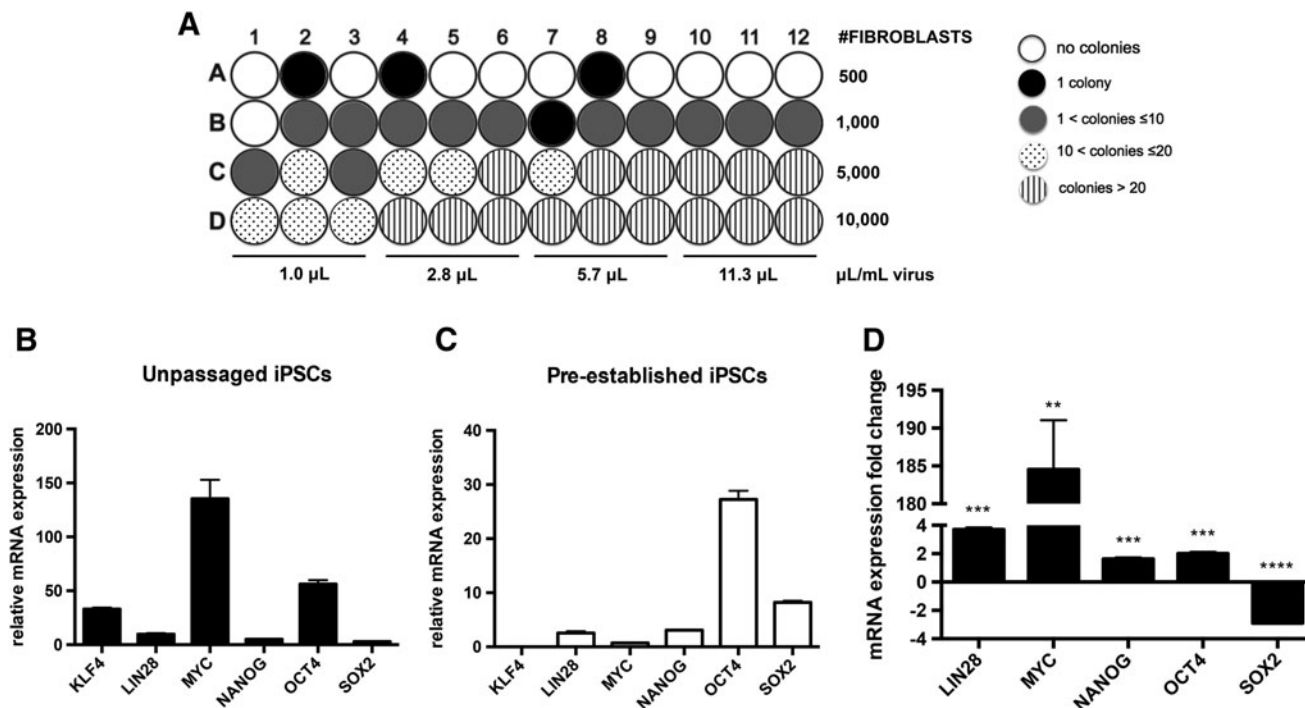


**FIG. 3.** Skin fibroblasts reprogram in 96-well plate using 1.0 µL Sendai virus per well. Human primary skin fibroblasts at passage 6 were seeded at four different concentrations. On the following day, a serial dilution of 1.0, 2.8, 5.7, and 11.3 µL of Sendai virus was added. RT-qPCR were shown of gene expression levels of the pluripotency markers KLF4, LIN28, MYC, NANOG, OCT4, and SOX2. Expression levels were depicted as relative to HPRT. Significance was represented as  $*P < 0.05$ ,  $**P < 0.01$ ,  $***P < 0.001$ , and  $****P < 0.0001$ . (A) Visualization of the amount of iPSC colonies per well at reprogramming day 19 following a color scaling system: *white*, no colonies; *black*, 1 colony; *gray*, 1–9 colonies; *dots*, 10–19 colonies; *stripes*, 20 or more colonies. (B) Relative mRNA expression of pluripotency markers in the unpassaged iPSCs formed in the wells D7 to D11 of the 96-well plate shown in Fig. 3A. (C) Relative mRNA expression of pluripotency markers in preestablished iPSCs. (D) Gene expression levels of unpassaged iPSCs compared with gene expression levels of preestablished iPSCs depicted as fold change. The expression levels of each gene were quantified, normalized to B2M (reference gene), and the results are presented as mean  $\pm$  SEM. Significance was calculated with unpaired Student's *t*-test with Welch's correction if variances were not equal. HPRT, hypoxanthine guanine phosphoribosyl transferase; RT-qPCR, quantitative reverse transcription–polymerase chain reaction.

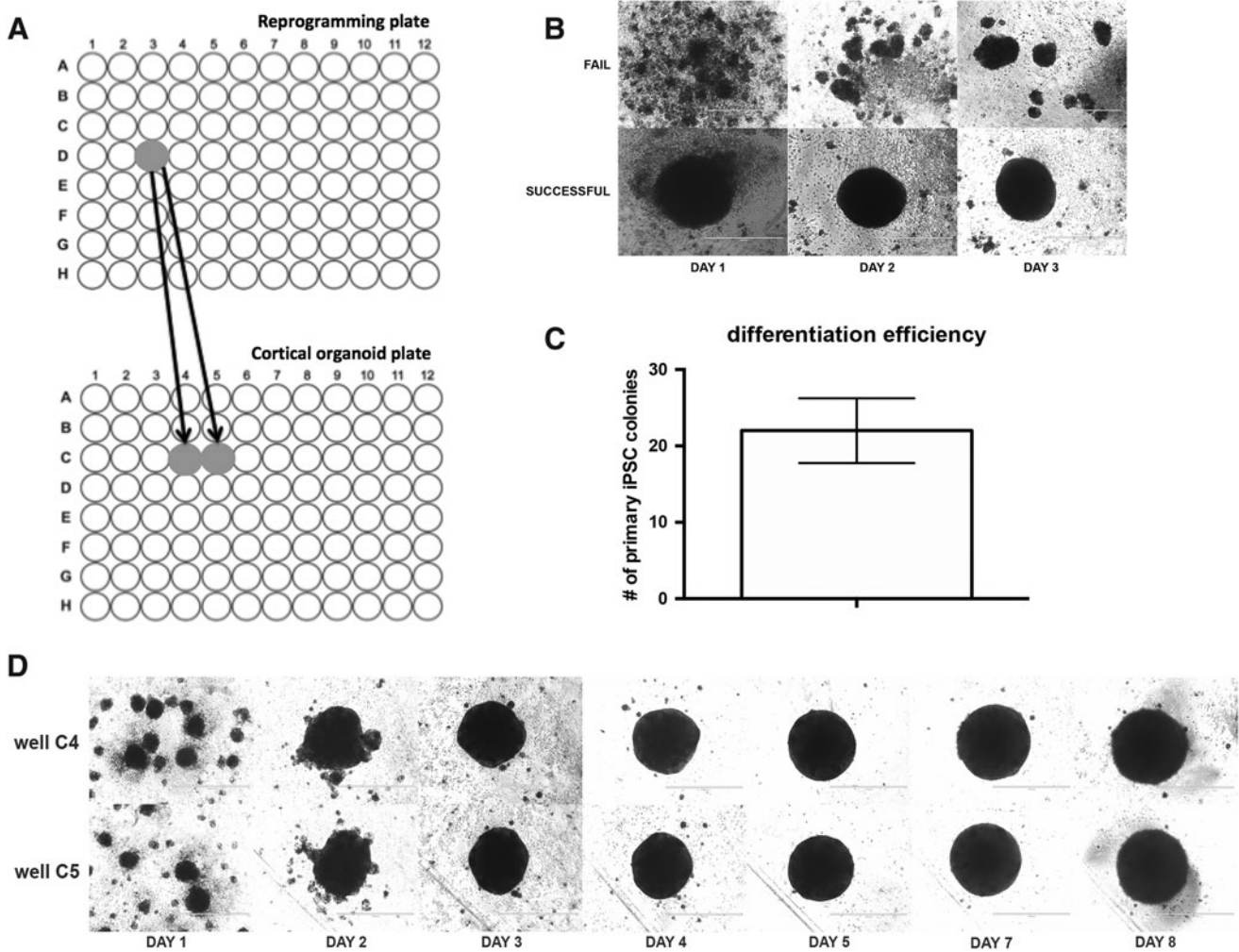


**FIG. 4.** Direct generation of cortical organoids from reprogrammed fibroblasts in a 96-well plate. Direct differentiation protocol in a 96-well plate using primary iPSC colonies that were formed in a 96-well plate. **(A)** One well of reprogrammed skin fibroblasts from the experiment of Fig. 3 was seeded to two wells of an ultralow attachment 96-well plate. The iPSCs were at reprogramming day 23. The cortical organoids protocol was followed as described in the Materials and Methods section. **(B)** *Top*: Unsuccessful organoid forming of the primary iPSC colonies. *Bottom*: Successful organoid forming of primary colonies showed in organoid formation starting between days 2 and 3. Scale bar, 1,000  $\mu\text{m}$ . **(C)** Relative amount of primary iPSC colonies in one well that successfully differentiated into two organoids. Data are shown as mean  $\pm$  SEM,  $n = 2$ . **(D)** Developing cortical organoids followed until day 8. Images were made using the EVOS microscope at magnification  $4\times$ . Scale bar, 1,000  $\mu\text{m}$ .

transduction facilitated iPSC survival. At day 19, the number of colonies as counted for each well was presented in Fig. 3A. Our results show that 5,000 fibroblasts and 1.0  $\mu\text{L}$  of Sendai virus per well gave rise to 2–20 healthy colonies.

The pluripotency state was verified by evaluating the gene expression levels of the pluripotency markers *KLF4*, *LIN28*, *MYC*, *NANOG*, *OCT4*, and *SOX2*, which we compared to the expression levels of a preestablished passaged iPSC line, previously generated as a control line (Fig. 3B). The Sendai virus kit contained *c-Myc*, *SOX2*, *OCT3/4*, and *KLF4*. As a result, it was expected that *KLF4*, *c-MYC*, *OCT4*, and *SOX2* would be highly expressed in the newly formed unpassaged iPSC colonies (Fig. 3B, D). *SOX2* showed to be significantly lower expressed compared to the preestablished iPSCs (Fig. 3C). Although *LIN28* and *NANOG* were not in the Sendai virus kit, their expression was also significantly higher compared with the preestablished iPSCs (Fig. 3D).

Next, we further optimized the protocol by using one reprogrammed well to form cortical organoids in another 96-well plate directly. We found that the best way to accomplish this was to seed one reprogrammed well into two wells and then start the cortical organoids protocol (Fig. 4A, B). Two organoids were formed with an average of 22 primary colonies (Fig. 4C). After only 3 days, cortical organoids started to emerge (Fig. 4D). Thus, even unpassaged iPSC with relatively high levels of some pluripotent genes could be induced to differentiate in our conditions.

## Discussion

In this study, we describe a rapid and cost-effective method to reprogram somatic cells and the direct generation of cortical organoids in a 96-well format. Our results suggested that the best condition is on 5,000 fibroblasts per well, infected with 1  $\mu\text{L}$

Sendai virus cocktail (hKOS, hKlf4 and hc.myc). Moreover, we found that seeding 5,000 MEFs directly into the reprogramming wells after transduction might slightly increase iPSC survival. It is difficult to assess if a single (clonal) or multiple (oligoclonal) cells were reprogrammed in our experimental condition. Thus, it is possible that iPSCs from each well represent a mosaic from different donor fibroblasts.

Although it was suggested that differentiation of iPSCs requires various passages to be successful [25–28], our work describes the direct differentiation of nonpassaged iPSCs into cortical organoids for the first time. By immunostaining, we showed the presence of both NPCs and neurons in the cortical organoids formed out of nonpassaged iPSCs. However, these same markers could also be found in embryoid bodies. To exclude that these spheres are embryoid bodies, a full characterization of brain organoids made by the same cortical organoid protocol, with cortical layer structure immunostaining as well as single-cell PCR analysis has been performed by Trujillo et al. [29]. We optimized the protocol by taking the nonpassaged iPSC colonies of 1 well and directly generating cortical organoids in 2 wells of another 96-well plate.

Finally, it is also possible that only partially reprogrammed cells could be further differentiated. In vitro lineage conversion of fibroblasts into NPCs has been shown using fibroblasts of mice [30–32] and humans [33–35]. In any case, further functional electrophysiological analyses will be required to characterize these cortical organoids.

The results described here show the basis of a protocol that can be automated to generate a large cohort of samples that could be used for different experimental assessment of genetically encoded human cognitive variability. Potential uses of these platforms include the generation of large brain organoid repositories and the discovery of causal genetic variants to human neurological conditions associated with several mutations of unknown significance such as ASD.

## Acknowledgments

This work was supported by grants from the National Institutes of Health through the R01MH094753, R01MH103134, U19MH107367, and a NARSAD Independent Investigator Grant to A.R.M.

## Author Disclosure Statement

Dr. Muotri is a cofounder and has an equity interest in TISMOO, a company dedicated to genetic analysis focusing on therapeutic applications customized for autism spectrum disorder and other neurological disorders with genetic origins. The terms of this arrangement have been reviewed and approved by the University of California San Diego following its conflict of interest policies. The other authors declare no conflicts of interest.

## References

- Ronald A and RA Hoekstra. (2011). Autism spectrum disorders and autistic traits: a decade of new twin studies. *Am J Med Genet B Neuropsychiatr Genet* 156B:255–274.
- Dolmetsch R and DH Geschwind. (2011). The human brain in a dish: the promise of iPSC-derived neurons. *Cell* 145: 831–834.
- Clowry G, Z Molnár and P Rakic. (2010). Renewed focus on the developing human neocortex. *J Anat* 217:276–288.
- Dragunow M. (2008). The adult human brain in preclinical drug development. *Nat Rev Drug Discov* 7:659–666.
- Oberheim NA, X Wang, S Goldman and M Nedergaard. (2006). Astrocytic complexity distinguishes the human brain. *Trends Neurosci* 29:547–553.
- Steffenhagen C, S Kraus, FX Dechant, M Kandasamy, B Lehner, AM Poehler, T Furtner, FA Siebzehrubl, S Couillard-Despres, et al. (2011). Identity, fate, and potential of cells grown as neurospheres: species matters. *Stem Cell Rev* 7:815–835.
- Takahashi K, K Tanabe, M Ohnuki, M Narita, T Ichisaka, K Tomoda and S Yamanaka. (2007). Induction of pluripotent stem cells from adult human fibroblasts by defined factors. *Cell* 131:861–872.
- Fatehullah A, SH Tan and N Barker. (2016). Organoids as an in vitro model of human development and disease. *Nat Cell Biol* 18:246–254.
- Negraes PD, FR Cugola, RH Herai, CA Trujillo, AS Cristino, T Chailangkarn, AR Muotri and V Duvvuri. (2017). Modeling anorexia nervosa: transcriptional insights from human iPSC-derived neurons. *Transl Psychiatry* 7: e1060.
- Chailangkarn T, CA Trujillo, BC Freitas, B Hrvov-Mihic, RH Herai, DX Yu, TT Brown, MC Marchetto, C Bardy, et al. (2016). A human neurodevelopmental model for Williams syndrome. *Nature* 536:338–343.
- Griesi-Oliveira K, A Acab, AR Gupta, DY Sunaga, T Chailangkarn, X Nicol, Y Nunez, MF Walker, JD Murdoch, et al. (2015). Modeling non-syndromic autism and the impact of TRPC6 disruption in human neurons. *Mol Psychiatry* 20:1350–1365.
- Eiraku M, N Takata, H Ishibashi, M Kawada, E Sakakura, S Okuda, K Sekiguchi, T Adachi and Y Sasai. (2011). Self-organizing optic-cup morphogenesis in three-dimensional culture. *Nature* 472:51–56.
- Lancaster MA, M Renner, CA Martin, D Wenzel, LS Bicknell, ME Hurles, T Homfray, JM Penninger, AP Jackson and JA Knoblich. (2013). Cerebral organoids model human brain development and microcephaly. *Nature* 501:373–379.
- Mariani J, MV Simonini, D Palejev, L Tomasini, G Coppola, AM Szekely, TL Horvath and FM Vaccarino. (2012). Modeling human cortical development in vitro using induced pluripotent stem cells. *Proc Natl Acad Sci U S A* 109:12770–12775.
- Paşca AM, SA Sloan, LE Clarke, Y Tian, CD Makinson, N Huber, CH Kim, JY Park, NA O'Rourke, et al. (2015). Functional cortical neurons and astrocytes from human pluripotent stem cells in 3D culture. *Nat Methods* 12:671–678.
- Lancaster MA and JA Knoblich. (2014). Generation of cerebral organoids from human pluripotent stem cells. *Nat Protoc* 9:2329–2340.
- Camp JG, F Badsha, M Florio, S Kanton, T Gerber, M Wilsch-Bräuninger, E Lewitus, A Sykes, W Hevers, et al. (2015). Human cerebral organoids recapitulate gene expression programs of fetal neocortex development. *Proc Natl Acad Sci U S A* 112:15672–15677.
- Wells MF, MR Salick, O Wiskow, DJ Ho, KA Worringer, RJ Ihry, S Kommineni, B Bilican, JR Klim, et al. (2016). Genetic ablation of AXL does not protect human neural progenitor cells and cerebral organoids from Zika virus infection. *Cell Stem Cell* 19:703–708.



19. Garcez PP, EC Loiola, RM Madeiro da Costa, LM Higa, P Trindade, R Delvecchio, JM Nascimento, R Brindeiro, A Tanuri and SK Rehen. (2016). Zika virus impairs growth in human neurospheres and brain organoids. *Science* 352: 816–818.
20. Cugola FR, IR Fernandes, FB Russo, BC Freitas, JL Dias, KP Guimarães, C Benazzato, N Almeida, GC Pignatari, et al. (2016). The Brazilian Zika virus strain causes birth defects in experimental models. *Nature* 534:267–271.
21. Thomas CA, L Tejwani, CA Trujillo, PD Negraes, RH Herai, P Mesci, A Macia, YJ Crow and AR Muotri. (2017). Modeling of TREX1-dependent autoimmune disease using human stem cells highlights L1 accumulation as a source of neuroinflammation. *Cell Stem Cell* 21:319–331.e8.
22. MacArthur CC, A Fontes, N Ravinder, D Kuninger, J Kaur, M Bailey, A Taliana, MC Vemuri and PT Lieu. (2012). Generation of human-induced pluripotent stem cells by a nonintegrating RNA Sendai virus vector in feeder-free or xeno-free conditions. *Stem Cells Int* 2012:564612.
23. Lai WH, JC Ho, YK Lee, KM Ng, KW Au, YC Chan, CP Lau, HF Tse and CW Siu. (2010). ROCK inhibition facilitates the generation of human-induced pluripotent stem cells in a defined, feeder-, and serum-free system. *Cell Reprogram* 12:641–653.
24. Chung HC, RC Lin, GJ Logan, IE Alexander, PS Sachdev and KS Sidhu. (2012). Human induced pluripotent stem cells derived under feeder-free conditions display unique cell cycle and DNA replication gene profiles. *Stem Cells Dev* 21:206–216.
25. Koehler KR, P Tropel, JW Theile, T Kondo, TR Cummins, S Viville and E Hashino. (2011). Extended passaging increases the efficiency of neural differentiation from induced pluripotent stem cells. *BMC Neurosci* 12:82.
26. Polo JM, S Liu, ME Figueroa, W Kulalert, S Eminli, KY Tan, E Apostolou, M Stadtfeld, Y Li, et al. (2010). Cell type of origin influences the molecular and functional properties of mouse induced pluripotent stem cells. *Nat Biotechnol* 28:848–855.
27. Kim K, A Doi, B Wen, K Ng, R Zhao, P Cahan, J Kim, MJ Aryee, H Ji, et al. (2010). Epigenetic memory in induced pluripotent stem cells. *Nature* 467:285–290.
28. Marchetto MCN, GW Yeo, O Kainohana, M Marsala, FH Gage and AR Muotri. (2009). Transcriptional signature and memory retention of human-induced pluripotent stem cells. *PLoS One* 4:e7076.
29. Trujillo CA, R Gao, PD Negraes, IA Chaim, A Domissy, M Vandenberghe, A Devor, GW Yeo, B Voytek and AR Muotri. (2018). Nested oscillatory dynamics in cortical organoids model early human brain network development. *bioRxiv*. [Epub ahead of print]; DOI: <https://doi.org/10.1101/358622>.
30. Lujan E, S Chanda, H Ahlenius, TC Südhof and M Wernig. (2012). Direct conversion of mouse fibroblasts to self-renewing, tripotent neural precursor cells. *Proc Natl Acad Sci U S A* 109:2527–2532.
31. Thier M, P Wörsdörfer, YB Lakes, R Gorris, S Herms, T Opitz, D Seiferling, T Quandel, P Hoffmann, et al. (2012). Direct conversion of fibroblasts into stably expandable neural stem cells. *Cell Stem Cell* 10:473–479.
32. Kim J, JA Efe, S Zhu, M Talantova, X Yuan, S Wang, SA Lipton, K Zhang and S Ding. (2011). Direct reprogramming of mouse fibroblasts to neural progenitors. *Proc Natl Acad Sci U S A* 108:7838–7843.
33. Connor B, E Firmin, C Mauck, R Liu, R Playne, K Jones and M Dottori. (2015). Direct conversion of adult human fibroblasts into induced neural precursor cells by non-viral transfection. *Protoc Exch*[Epub ahead of print]; DOI: 10.1038/protex.2015.034.
34. Mitchell RR, E Szabo, YD Benoit, DT Case, R Mechael, J Alamilla, JH Lee, A Fiebig-Comyn, DC Gillespie and M Bhatia. (2014). Activation of neural cell fate programs toward direct conversion of adult human fibroblasts into tripotent neural progenitors using OCT-4. *Stem Cells Dev* 23: 1937–1946.
35. Yu KR, JH Shin, JJ Kim, MG Koog, JY Lee, SW Choi, HS Kim, Y Seo, S Lee, et al. (2015). Rapid and efficient direct conversion of human adult somatic cells into neural stem cells by HMGA2/let-7b. *Cell Rep* 10:441–452.

Address correspondence to:

*Dr. Alysson R. Muotri*

*Department of Pediatrics*

*Rady Children's Hospital San Diego*

*University of California San Diego School of Medicine*

*2880 Torrey Pines Scenic Drive, MC0695*

*La Jolla, CA 92037*

*E-mail: muotri@ucsd.edu*

Received for publication May 29, 2018

Accepted after revision August 24, 2018

Prepublished on Liebert Instant Online August 24, 2018